Title: Articular cartilage corefucosylation regulates tissue resilience in osteoarthritis

Short title: Articular cartilage corefucosylation and tissue resilience in OA

Kentaro Homan[1], Tomohiro Onodera[1]*, Hisatoshi Hanamatsu[2], Jun-ichi Furukawa[1, 2], Daisuke Momma[3], Masatake Matsuoka[1], Norimasa Iwasaki[1]

[1] Department of Orthopaedic Surgery, Faculty of Medicine and Graduate School of Medicine, Hokkaido University, Kita 15, Nishi 7, Kita-ku, Sapporo 060-8638, Japan

[2] Institute for Glyco-core Research (iGCORE), Nagoya University, Nagoya 464-8601, Japan

[3] Center for Sports Medicine, Hokkaido University Hospital, Kita 14, Nishi 5, Sapporo 060-8638, Japan.

*Corresponding author: Tomohiro Onodera

Department of Orthopaedic Surgery, Faculty of Medicine and Graduate School of Medicine

Hokkaido University, Kita 15, Nishi 7, Kita-ku, Sapporo 060-8638, Japan

Telephone: +81-11-706-2111

Email: tomozou@med.hokudai.ac.jp

Abstract

This study aimed to investigate the glycan structural changes that occur before histological degeneration in osteoarthritis (OA) and to determine the mechanism by which these glycan conformational changes affect cartilage degeneration. An OA model was established in rabbits using mannosidase injection, which reduced high-mannose type N-glycans and led to cartilage degeneration. Further analysis of glycome in human OA cartilage identified specific corefucosylated N-glycan expression patterns. Inhibition of N-glycan corefucosylation resulted in unrecoverable cartilage degeneration, while cartilage-specific blocking of corefucosylation led to accelerated development of aging-associated and instability-induced OA models. We conclude that α1,6 fucosyltransferase is required postnatally to prevent preosteoarthritic deterioration of articular cartilage. These findings provide a novel definition of early OA and identify glyco-phenotypes of OA cartilage, which may distinguish individuals at higher risk of progression.

Keywords: early osteoarthritis, glyco-phenotypes, α1,6 fucosyltransferase, cartilage glycome

INTRODUCTION

Osteoarthritis (OA), a degeneration of joint components, such as proteoglycans (PGs) and collagen, destroys cartilage and impairs joint function (1). The global prevalence of OA is estimated to be >500 million, which is a significant socioeconomic burden (2). Therefore, preventive measures must be implemented to reduce the future disease burden and disability. Once the cartilage is destroyed, it cannot be repaired homogeneously and progresses irreversibly thereafter (3, 4). Since articular cartilage has no blood vessels and is not innervated, it is difficult for symptoms to appear. By the time clinical symptoms appear, the condition is often already considerably advanced (5). Therefore, from a preventive

46 perspective, it is necessary to define and detect "pre-OA," the stage before the onset of early
47 OA (6, 7). Pre-OA is a knee with no pain, no motor function problems, and no arthroscopic or
48 structural changes on radiography, only emerging cellular effects. Despite many studies, there
49 is no gold standard for OA biomarkers (8). It is important to characterize the disease state
50 before OA to shift the paradigm from mitigation to late-onset disease prevention.
51 In the very early stages of OA, before cartilage matrix degeneration, cartilage destruction by
52 enzymatic processes that degrade glycoproteins, PGs, and collagen, in that order, is underway
53 (9). Collagenolytic activity is largely unchanged on intact articular surfaces (10, 11), and
54 glycoprotein degradation is thought to be an early transient event in the enzymatic process of
55 cartilage destruction because hexose degradation of glycoproteins promotes degradation of
56 the protein portion of the molecule by proteinases (12). Additionally, cartilage damage is
57 reversible if type 2 collagen breakdown is mild (13). Structural change analysis in
58 glycoproteins is necessary for the early stages of OA but has not yet been performed
59 sufficiently.
60 Matsuhashi *et al*.'s study showed that structural changes in N-glycans occurred in
61 degenerated cartilage in a rabbit OA model before tissue changes occurred (14). Urita *et al*.
62 demonstrated that these N-glycans in degenerated mice and human cartilage are high-
63 mannose type N-glycans (15). Furthermore, among several glycosidases, mannosidase
64 activity was very high in OA joints, and its activity was high before the progression of
65 cartilage fibrosis (16). This suggests that high-mannose type N-glycan plays an important
66 role in OA pathogenesis. However, whether changes in the glycan structure are involved in
67 OA pathogenesis is unclear.
68 This study analyzed the glycan structural changes that preceded OA degeneration and
69 elucidated the mechanism of glycan structural changes in cartilage degeneration. For this
70 purpose, the effects of mannosidase, a specific degrading enzyme of high-mannose type N-

71 glycans associated with OA, on cartilage tissues and its molecular mechanisms were
72 analyzed.
73
74 **RESULTS**
75 **Mannosidase injection caused early OA-like change in vivo**
76 A decrease in Safranin O staining in the right femoral condyle of the α-mannosidase-injected
77 knee after 4 weeks was observed (Fig. 1A, B). Terminal deoxynucleotidyl transferase dUTP
78 nick end labeling (TUNEL) staining was enhanced in the superficial layer compared with that
79 in control. Articular cartilage chondrocytes exposed to α-mannosidase were not arranged in
80 columns in the middle zone. The surfaces of each group were smooth and had a good
81 macroscopic appearance (Fig. 1C). None of the groups showed a decrease in type 2 collagen
82 staining, and the orientation was maintained (Fig. 1D). To achieve optimal activity, the pH
83 range of 4 to 5 is ideal for mannosidase. In a physiological saline solution with a pH of 7 and
84 a concentration of 100 μg/ml, it exhibited specific activity. Nevertheless, at a concentration of
85 1.0 μg/ml, this activity was no longer present (S1 Figure). The mean histological score of the
86 α-mannosidase group was 0.83, indicating mild OA (Fig. 1E). The control group was
87 unchanged. Cartilage degeneration during intermittent intra-articular administration of
88 mannosidase was reversed upon discontinuation (Fig. 1F).
89
90 **Depletion of high-mannose type N-glycans in chondrocytes leads to cartilage**
91 **degradation ex vivo**
92 To quantify the degeneration and resilience promoted by the injection of α-mannosidase, the
93 cultured cartilage was harvested at different time points (Fig. 2A). Concanavalin A (Con A)
94 reactivity declined in articular cartilage treated with α-mannosidase (Fig. 2B). The
95 application of α-mannosidase stimulated the release of PG from cultured cartilage in

96 association with extracellular matrix degradation (Fig. 2C) and showed significantly higher
97 spontaneous nitric oxide (NO) release than the control over time (Fig. 2F). Mannosidase-
98 exposed cartilage showed an increase in TUNEL-positive cells in chondrocytes in the deep
99 zone and type 10 collagen-positive cells in superficial chondrocytes; however, these changes
100 did not occur in cytokine-stimulated cartilage (S2 Figure). Mannosidase exposure increased
101 *Adamts5* expression and suppressed *Mmp13* expression and anabolic factors (Fig. 3E). In the
102 articular cartilage that was exposed to freeze-thaw treatment before culture, no differences in
103 PG loss were observed between the α-mannosidase-stimulated cartilage and non-stimulated
104 cartilage (Fig. 2E). Excluding mannosidase loading, PG leakage and Safranin O staining were
105 restored (Fig. 2D), but Con A staining loss was not. Sialidase addition did not cause PG
106 leakage or NO production (S3 Figure), and the aggrecan lost in the catabolic phase was not
107 replenished in the subsequent anabolic phase.
108
109 **Corefucosylated N-glycan was formed in resilient cartilage and isolated chondrocyte**
110 Glycoblotting analysis revealed a significant difference in the N-glycan profiles (Fig. 3A and
111 S1 Table). Plotting m/z after mannosidase exposure against m/z before mannosidase exposure
112 demonstrated that only N-glycans were affected by enzyme dissociation from the y = x line
113 (Fig. 3B, S2 Table). In both denatured and reverted cartilages, Man8-9GlcNAc2 was
114 decreased, and Man5-6GlcNAc2 was increased by the action of mannosidase, which has a
115 high specificity for the terminal mannosidic residues of glycans (Fig. 3C, D). In contrast,
116 corefucosylated N-glycans, which were formed in the same biosynthesis pathway, were also
117 found (Fig. 3D). Similarly, the N-glycan profiles of isolated chondrocytes showed the
118 presence of this corefucosylated structure (S4 Figure). The expression of *Fut8*, the only
119 enzyme involved in corefucosylation, increased significantly in mannosidase-treated cartilage
120 (Fig. 3E).

121

122 **Deficiency of corefucosylated glycans in articular cartilage inhibits recovery from**

123 **cartilage damage and promotes cartilage degeneration**

124 We first examined whether the absence of core fucose affects the resilience of cartilage

125 degeneration. Mice lacking *Fut8* exhibited severe growth retardation and died shortly after

126 birth. Therefore, we decided to generate *Fut8* conditional knockout (cKO) mice (Fig. 4A, B).

127 The tissue specificity of recombination was confirmed by polymerase chain reaction (PCR)

128 analysis of mouse genomic DNA that detected either the intact $Fut8^{loxP}$ allele or the Cre-

129 recombined $Fut8^{\Delta}$ allele in repeated crosses; N-glycan analysis of cartilage demonstrated the

130 loss of corefucosylated sugar chains (Fig. 4C). The proportion of high-mannose type N-

131 glycan content was unchanged in cartilage lacking the *Fut8* gene (S5 Figure). Next, we used

132 real-time (RT)-PCR to determine relative *Fut8* messenger (m)-RNA levels in the cartilage of

133 Col2-$Fut8^{-/-}$ mice and their wild-type (WT) littermates ($Fut8^{loxP/loxP}$). Real-time polymerase

134 chain reaction (RT-PCR) analysis showed that *Fut8* mRNA expression was reduced by >99%

135 in the articular cartilage of Col2-$Fut8^{-/-}$ mice compared to that in their WT littermates ($P <$

136 0.01; $n = 3$ mice per group) (Fig. 4D). Chondrocyte-surface corefucosylation levels were

137 analyzed by lectin staining using *Pholiota squarrosa* lectin (PhoSL), which specifically

138 recognizes α1-6 core fucose (17). PhoSL lectin staining was completely absent in the articular

139 cartilage of *Fut8* cKO mice, in contrast to the positive staining observed in *Fut8* flox mice

140 under physiological conditions (Fig. 4E). Enzymatic degradation of high-mannose type N-

141 glycans on the cartilage in *Fut8*-deficient mice exacerbated cartilage degeneration (Fig. 4E,

142 F). In addition, reversible matrix repair by enzyme removal observed in control cartilage was

143 not observed in *Fut8*-deficient cartilage explant cultures. To evaluate whether TGF-β1

144 decreases cartilage degeneration after mannosidase stimulation, TGF-β1 was exogenously

145 added to Col2-$Fut8^{-/-}$ cartilage in the presence of α-mannosidase stimulation for 24 h. The

146 samples treated with TGF-β1 leaked significantly less PG following mannosidase stimulation
147 compared to samples not treated with TGF-β1 (Fig. 4F).
148
149 **Loss of corefucosylated glycans in articular cartilage leads to premature OA**
150 Col2-*Fut8*$^{-/-}$ mice developed and grew normally without major organ abnormalities of major
151 organs and could not be distinguished from their WT littermates. The whole skeletons of
152 newborn mice stained with alcian blue and alizarin red did not differ in appearance between
153 the genotypes (Fig. 5A). Col2-*Fut8*$^{-/-}$ mice showed a lower body weight than their WT
154 littermates, as indicated by the growth curve (Fig. 5B). To assess the role of FUT8 in
155 endochondral ossification, we performed an epiphyseal plate analysis of 4-week-old Col2-
156 *Fut8*$^{-/-}$ mice. This uncovered a significant enlargement of the zone of hypertrophic
157 chondrocytes in the growth plates of the long bones of Col2-*Fut8*$^{-/-}$ mice compared to
158 controls (Fig. 5C, S6 Figure). We analyzed the development of instability-induced OA
159 changes in *Fut8*$^{\mathrm{loxP/loxP}}$ and *Fut8* cKO mice. Sham operations produced no significant changes
160 in OA in either mouse genotype. Eight weeks after instability-inducing surgery, the joints of
161 WT mice developed changes in OA, such as cartilage erosion and a reduction in Safranin O
162 staining and chondrocyte number. Deletion of FUT8 results in more severe changes in OA. In
163 the joints of *Fut8* cKO mice, 8 weeks after surgery, the noncalcified zone (the upper layer
164 above the tidemark) was almost completely lost. The number of chondrocytes was
165 significantly reduced (Fig. 5D). Quantitative assessment using the OA Research Society
166 International (OARSI) score supported these histological findings (difference: -2.900;
167 *Fut8*$^{flox/flox}$/destabilization of the medial meniscus (DMM) versus *Col2a1-Cre*;
168 *Fut8*$^{flox/flox}$/DMM, 95% confidence interval [CI] for the difference: -5.027 to -0.7734) (Fig.
169 5E). Changes in OA progressed earlier in the aging models of *Fut8*-deficient mice than in
170 control mice (WT and floxed mice). The mice were followed up until 15 months of age to

171 assess the spontaneous development of OA with aging (Fig. 5F). There were no apparent
172 changes of OA in the knee joints of either mouse genotype at 3 months of age (Fig. 5G). At 4
173 months of age, significant changes in OA were detected in the knee joints of the *Fut8* cKO
174 mice. The cartilage surface integrity was no longer maintained at 9 months. These OA
175 changes progressed more in *Fut8* cKO mice than in their WT littermates at 15 months. These
176 histological findings were quantitatively confirmed by the Osteoarthritis Research Society
177 International (OARSI) scores (difference: -2.000; WT versus *Col2a1-Cre; Fut8*$^{flox/flox}$, 95% CI
178 for the difference: -3.723 to -0.2771 at 4 months, difference: -2.700; WT versus *Col2a1-Cre;*
179 *Fut8*$^{flox/flox}$, 95% CI for the difference: -4.423 to -0.9771 at 9 months, and difference: -6.700;
180 WT versus *Col2a1-Cre; Fut8*$^{flox/flox}$, 95% CI for the difference: -8.423 to -4.977 at 15
181 months).
182
183 **Altered glycosylation of human OA cartilage based on comprehensive glycan analysis**
184 Total glycome profiling of human OA cartilage is shown in Fig. 6A and S3 Table. The
185 amount of high-mannose type N-glycan was significantly decreased, the same as previously
186 reported in OA cartilages (Fig. 6A) (15). Focusing on fucosylation, most of the
187 complex/hybrid type glycans were modified with fucose. The fucosylation that occurs at the
188 innermost N-acetylglucosamine (GlcNAc) of N-glycans could be recognized with a lectin
189 from the mushroom Pholiota squarrosa (PhoSL) and was able to detect the expression of the
190 corefucose structure. Therefore, we suspected that the stainability of PhoSL is increased in
191 OA cartilage. As expected, the PhoSL staining of OA cartilage was significantly increased
192 relative to that of a healthy control (Fig. 6B). We performed principal component analysis
193 (PCA) on 1110 glycomic data, discriminating OA from healthy cartilages along the first
194 principal component (PC1) axis (Fig. 6C). Hierarchical cluster analysis showed that clades
195 containing corefucosylated glycans were clustered (Fig. 6D), and N-13 ((Hex)1 (HexNAc)1

196 (Fuc)1 + (Man)3(GlcNAc)2) has the largest squared correlation with its cluster component.

197

198 **DISCUSSION**

199 The objective of this work was to provide novel and translational insights into the
200 pathogenesis of OA associated with changes in glycan structure. A graphical abstract
201 summarizing our findings is shown in Fig. 7. To test the hypothesis that structural changes in
202 high-mannose type N-glycans may induce OA, we tested the effect of mannosidase loading
203 on the structure of high-mannose type N-glycans. Consequently, modifying the structure of
204 high-mannose type N-glycans by mannosidase loading induced OA-like histological
205 alterations. Furthermore, the OA-like changes induced by mannosidase were recovered by
206 enzyme removal. These results suggest that structural alterations of high-mannose type N-
207 glycans lead to OA-like histological changes in articular cartilage but do not necessarily
208 cause the pathogenesis of eventual OA. Subsequently, glycoblotting analysis revealed that
209 core-fucose-containing glycans underwent complementary structural alterations per high-
210 mannose type N-glycans. This suggests that the structural change of core-fucose-containing
211 glycans may have some compensatory mechanism for OA-like alterations caused by the
212 structural change of high-mannose type N-glycans. Furthermore, under the regulation of *Fut8*
213 expression, which regulates the synthesis of core fucose, mannosidase was found to induce
214 irreversible OA. The high-mannose/corefucosylation relationship estimated function to
215 maintain formed cartilage. In endochondral ossification, the *Fut8* cKO growth plate had an
216 enlarged hypertrophic zone and reduced primary spongiosa because it is involved in the next
217 process of cartilage replacement into bone rather than the process of cartilage formation.
218 These results provide the first evidence that structural alterations in glycans in the articular
219 cartilage regulate eventual OA development.

220 Two key targets of cartilage degeneration during OA are type II collagen, a major substrate of

221 matrix metalloproteinase (MMP)-13 (18), and aggrecan, a PG with glycosaminoglycan side
222 chains of chondroitin and keratin sulfate (19, 20). The degradation of non-collagenous
223 molecules, such as aggrecan, occurs before the degradation of type II collagen in the early
224 stages of OA (20, 21). The histological analysis in this study revealed that the alteration in the
225 structure of high-mannose type N-glycans resulted in a decrease in Safranin O staining (a
226 decrease in glycosaminoglycans and/or PGs), whereas there was no change in collagen
227 staining. These findings are consistent with alterations in the early stages of OA.
228 Furthermore, we observed that removing mannosidase could cause PG loss to the control
229 level. Karsdal *et al.* demonstrated that articular cartilage degradation is reversible in the
230 presence of aggrecanase and concluded that the repair ability is not impaired before the
231 degradation of aggrecan and type II collagen by MMPs (22). Reimann *et al.* observed that the
232 glycosaminoglycans loss in articular cartilage is reversible and an early sign of OA before the
233 "state of no return." (23) The present results are consistent with the findings of previous
234 reports on early OA and suggest that the mannosidase-loaded model can be considered an
235 early OA-like alteration.
236 Since the structural change in high-mannose type N-glycans alone did not cause irreversible
237 OA, we investigated other regulatory mechanisms related to high-mannose type N-glycans
238 that could induce irreversible OA. The expression of corefucosylated N-glycans on a series of
239 biosynthetic pathways was upregulated with structural changes in high-mannose type N-
240 glycans. FUT8 is known to corefucosylate small oligomannose N-glycans (Man4-
241 Man5GlcNAc2) but not large oligomannose N-glycans, such as Man8-Man9GlcNAc2 (24).
242 This suggests that small oligomannose N-glycans trimmed by mannosidase could activate
243 *Fut8*. *Fut8* is also upregulated in human OA chondrocytes (25, 26), and increased expression
244 of these corefucosylated N-glycans has been observed during late chondrocyte differentiation
245 (27). These findings suggested that these structural changes are related to OA-related

246 glycosylation.

247 To clarify the relationship between the alteration of corefucosylated N-glycans and cartilage
248 degeneration, *Fut8* cKO mice were used. Since the results of the ex vivo freeze-thaw model
249 showed that cartilage degeneration was induced by changes in the glycan structure of
250 chondrocytes, we used chondrocyte-specific KO mice. As a result, the reversibility of the
251 cartilage degeneration model was diminished. This finding suggests that *Fut8*-mediated
252 corefucosylation in chondrocytes plays a function in promoting glycan repair. Furthermore, to
253 directly determine whether *Fut8* was involved in the inhibition of OA progression, the OA
254 model was investigated. For the modeling of OA in *Fut8* cKO mice, the instability-induced
255 OA model and the age-associated OA model were adapted. The former emphasizes
256 mechanical stress factors in OA, the latter aging factors. OA is a multifactorial disease.
257 Therefore, we thought it was appropriate to validate both aspects of OA. The results showed
258 that conditional KO of *Fut8* in chondrocytes hastened the onset of OA. This suggests that
259 cartilage corefucosylation associated with FUT8 plays a protective role against the
260 attenuation of type II collagen in the OA process.

261 Finally, the expression of α1,6-linked core fucose on N-glycans in human cartilage is
262 associated with OA, and corefucosylation was found to be one of the characteristics in OA
263 cartilage. Total cellular glycome analysis, including N- and O-linked glycans derived from
264 glycoproteins, GSL-glycans, GAGs, and fOSs, is informative for analyzing cell-specific
265 characteristics (28–30). Glycome profiling enabled the detection of corefucosylated N-
266 glycans by sequential clustering of degenerated cartilage characteristics. Core fucose
267 deficient mice generated by ablating the α1,6 fucosyltransferase enzyme, FUT8, were
268 reported to have suppressed phosphorylation of Smad and increased expression of MMPs
269 (matrix metalloproteinases) due to decreased binding of TGF-β ligand caused by the lack of
270 core fucose addition to the TGF-β type II receptor (31, 32). The present study shows that

271 treatment of cartilage with mannosidase caused corefucosylation, suppression of *Mmp13*, and
272 increased expression of *Tgf-β*. Moreover, treatment of FUT8-knockout cartilage with
273 mannosidase resulted in the suppression of *Tgf-β* expression and increased *Mmp13*
274 expression. Here, the exogenous addition of TGF-β1 rescued them from cartilage
275 degeneration. These results suggest that corefucosylation following the loss of high-mannose
276 type N-glycans may provide chondroprotective effects via the TGF-β signaling pathway,
277 which may have been lost by FUT8-knockout.
278 One limitation of this study was that we did not have access to cartilage samples from
279 immediately before the onset of OA; thus, we do not know the expression of Fut8 in human
280 cartilage in the early stage of OA onset and its influence on extracellular matrix degradation
281 under homeostatic conditions. Obtaining cartilage specimens continues to be challenging,
282 especially for those with early stages of OA.
283 In summary, we show for the first time a key role of FUT8 and glycan-dependent signaling
284 mediators in extracellular matrix resilience associated with cartilage corefucosylation during
285 early OA.
286
287 **METHODS**
288 **Intra-articular injection of α-mannosidase in the knee**
289 We injected mannosidase into rabbit knee joints in accordance with a previous paper showing
290 that N-type glycans are altered prior to cartilage matrix degeneration. Japanese White rabbits
291 weighing 3.10 ± 0.15 kg purchased from a professional breeder (Japan SLC Inc., Hamamatsu,
292 Japan) were used for this study according to established ethical guidelines approved by the
293 local animal care committee. Animals were anesthetized with 10 mg/kg of intravenous
294 ketamine, followed by isoflurane in oxygen gas. Both knees in each rabbit were shaved,
295 prepared, and draped in a sterile fashion. α-Mannosidase from Canavalia ensiformis (Jack

296 bean) (Sigma, St Louis, MO, USA) was dissolved in saline. Five hundred microliter volumes
297 containing 1.9 units per ml (0.05 mg) of mannosidase solution were injected into the joint
298 cavity of the right knee. α-Mannosidase from Canavalia ensiformis (Jack bean) has been
299 widely used as a tool for glycan analysis, which has a high specificity towards terminal
300 mannosidic residues of glycans and participates in mannose trimming reactions (33). The
301 measurement of its performance in a saline solution was evaluated using the QuantiChrom α-
302 Mannosidase Assay Kit (BioAssay Systems, Hayward, CA, USA). This colorimetric assay
303 uses 4-nitrophenyl-α-d-mannopyranoside as a substrate to identify the generation of 4-
304 nitrophenol. The following doses of α-Mannosidase were administered: 0.5 ml at 0.01 μg/ml,
305 1.0 μg/ml, or 100 μg/ml. Simultaneously, the contralateral knee joint received an equal
306 volume of saline solution. Each joint was injected once or four times in alternate weeks. The
307 animals were euthanized at 4 and 16 weeks postoperatively. Each section of the knee joint
308 was stained with hematoxylin and eosin or Safranin O/fast green, as well as with
309 immunohistochemical staining for type II collagen and TUNEL. Two investigators quantified
310 the OA severity using the OARSI scoring method.
311
312 **Evaluation of collagen orientation by a polarized light microscope**
313 To evaluate the collagen orientation of the repaired tissue at 16 weeks postoperatively, a
314 supplemental evaluation using a polarized light microscope (PLM) (ECLIPSE E600 POL;
315 Nikon, Tokyo, Japan) was conducted (34). This evaluation was performed on HE-stained
316 sections from each group. Two cross polarizers were used so that highly ordered collagen
317 perpendicular to the articular surface appeared bright, while collagen that was not ordered
318 (nonbirefringent) appeared dark. The contrast of fibrils more parallel to the articular surface
319 was darker than collagen oriented perpendicular to the articular surface. To observe the
320 predominant direction of the birefringent regions and confirm the lack of orientation in the

321 nonbirefringent regions, the sections were rotated at 0°, 45°, and 90° for the fixed filters.
322 Microscopic images were acquired using a digital camera (DS-5M-L1, Nikon, Tokyo, Japan).
323 Each sample was examined independently by an experienced PLM user.
324
325 **Ex vivo analysis of deletion of high-mannose type N-glycan in cartilage**
326 Organ culture experiments in mice were established to study the effects of mannosidase on
327 articular cartilage without immunoreaction and in anticipation of later candidate gene
328 research using transgenic mice. According to the established ethical guidelines approved by
329 the local animal care committee, cartilage catabolism was analyzed by culturing femoral head
330 cartilage of 4-week-old C57BL6 male mice with α-mannosidase (1.9 U/mL) ex vivo (35, 36).
331 Mannosidase was removed on day 3, and organ culture was continued until day 6. To
332 evaluate cartilage degradation, quantification of PG release from cartilage explants was
333 performed using the dimethylmethylene blue assay (36, 37) and exposure to sialidase (1.9
334 U/mL) and interleukin-1 beta (Cat #. 300-01A; BioLegend, San Diego, CA, USA) (10
335 ng/mL) was also used as another control. The NO concentration in the culture medium was
336 measured using the Griess reagent system (Promega, Tokyo, Japan). To determine the direct
337 effects of mannosidase on the matrix, some cartilage explants were subjected to freeze-thaw
338 cycles in liquid nitrogen to destroy chondrocytes present in the superficial layer of the
339 cartilage (22, 38). After the procedure, the cells were replaced with the same culture medium
340 described above. Each tissue sample was stained with Safranin O. Lectin staining with Con A
341 (Wako Pure Chemical Industries, Richmond, VA, USA) and PhoSL (J-Oil Mills Inc., Tokyo,
342 Japan) was used to detect the high-mannose type N-glycans. Staining was performed using
343 the ABC Kit (Vector Labs, Burlingame, CA, USA), and the sections were counterstained with
344 HE.
345

346 **RNA extraction and quantitative RT-PCR analysis**

347 Total RNA was extracted from the samples using an RNeasy Mini Kit (Qiagen, Hilden,
348 Germany). For complementary DNA synthesis, 1.0 μg of RNA was reverse transcribed using
349 random hexamer primers (Promega, Tokyo, Japan) and ImProm II reverse transcriptase
350 (Promega). Quantitative RT-PCR was performed using a Thermal Cycler Dice Real Time
351 System II (Takara Bio Inc., Otsu, Japan) and SYBR Premix Ex Taq II (Takara, Shiga, Japan)
352 with gene-specific primers (S4 Table) in 15 μl of the mixture, following the manufacturer's
353 instructions. Quantitative data were normalized using peptidylprolyl isomerase A as an
354 endogenous reference gene and were calculated using the ΔΔCt method (39).

355

356 **Generation of *Fut8*$^{loxp/loxp}$*Col2a1-Cre* cKO mice**

357 *Fut8*$^{loxp/loxp}$ mice were provided by Tohoku Pharmaceutical University (Sendai, Japan). To
358 interrupt the synthesis of corefucosylated N-glycans in cartilage, we generated mice with
359 knockout of the chondrocyte-specific *Fut8* gene (Col2-*Fut8*$^{-/-}$ mice) by crossing *Fut8*$^{loxp/lox}$
360 mice with Col2a1-Cre–transgenic mice (40), in which Cre recombinase is expressed
361 specifically in chondrocytes under the Col2a1 promoter. Transgenic mice carrying the
362 Col2a1-Cre transgene (strain B6; SJL-Tg [Col2a1-Cre] 1Bhr/J; stock number 003554) were
363 obtained from the Jackson Laboratory (Bar Harbor, ME, USA). Homozygous *Fut8*$^{loxp/loxp}$
364 mice were bred with *Col2a1-Cre* mice, and offspring with the genotype *Fut8*$^{loxp/+}$ *Col2a1-*
365 *Cre* were bred with *Fut8*$^{loxp/loxp}$ mice to obtain the *Fut8*$^{loxp/loxp}$*Col2a1-Cre* cKO experimental
366 group and *Fut8*$^{loxp/loxp}$ (flox) littermate controls. All animals were maintained at Hokkaido
367 University under the regulations of the Institutional Animal Care and Use Committee.

368

369 **Skeletal examination**

370 To observe the skeletal systems, whole skeletons of WT and cKO littermates were stained

371 with alcian blue and alizarin red, as previously described (41, 42). The newborns were
372 skinned, eviscerated, and fixed in 95% ethanol. Intact skeletons were stained with 150 mg/ml
373 of alcian blue 8GX in 75% (vol/vol) ethanol/20% acetic acid for 24–48 hours and excess
374 tissues were removed by 1–2% KOH digestion for 2–3 days. The skeletal preparations were
375 stained with 75 mg/ml of alizarin red S in 1% KOH for 24 hours and cleared in graded
376 glycerol solutions (43).
377
378 **Instability-induced OA model**
379 An OA model was created in 10-week-old mice by destabilizing the knee joint as previously
380 described (44). With the mice under general anesthesia, we destabilized the right knee joint
381 by transection of the medial collateral ligament and removing the cranial half of the medial
382 meniscus using a microsurgical technique (DMM). A sham operation was performed on the
383 left knee joint using the same approach, without ligament transection and meniscectomy. For
384 histological assessment, the mice were sacrificed, and the entire knee joint was dissected 8
385 weeks postoperatively.
386
387 **Age-associated OA model**
388 At 3, 4, 9, and 15 months of age, the mice were sacrificed, and their entire knee joints were
389 dissected to assess the spontaneous development of OA as a model of age-associated OA (44,
390 45).
391
392 **Human Cartilage Preparation**
393 Acquisition and use of patient tissues were approved by the institutional review board (IRB)
394 of Hokkaido University (approval number: 014-0144), and informed consent was obtained in
395 advance. Samples were from patients undergoing total knee arthroplasty for clinically and

396 radiologically diagnosed OA (n=5; age range 61–84 years, mean 72.4; male: female ratio
397 1:4). Age-matched control articular cartilage was from patients undergoing total hip
398 arthroplasty for femoral neck fracture with no history of joint disease (n=5; age range 45–88
399 years, mean 61.2 years; male: female ratio 3:2). Each cartilage specimen was evaluated
400 macroscopically by at least two veteran doctors to ensure that it had not suffered damage or
401 degeneration and was treated within 9 hours of harvest in the operating room. Immediately
402 upon receipt, isolated human cartilage was homogenized with a Polytron blender
403 (Kinematica, Luzern, Switzerland), and then cold ethanol was added to separate the protein
404 and lipid fractions.
405
406 **Total cartilage glycomic analysis**
407 To determine whether the glycosylation detected is conserved across species, we analyzed the
408 total glycome in human cartilage. N-glycans were released directly using cartilage lysates
409 following deglycosylation by overnight treatment with peptide N-glycanase F (PNGase F,
410 2U) (Roche, Switzerland). The supernatants containing GSLs and fOSs were dried with a
411 centrifugal evaporator. GSL-glycans were isolated by enzymatic digestion using EGCase I
412 (Takara Bio Inc. Japan), whereas fOSs were recovered from an EGCase I-free fraction (46).
413 Cartilage lysate was delipidated and digested by GAG disaccharides (47). Extracted
414 glycoproteins were subjected to BEP for O-glycan analysis. Detailed procedures and
415 materials are provided elsewhere (48). N-glycans, fOSs, GAGs, and GSL-glycans were
416 subjected to glycoblotting (49). Purified N-glycans, fOSs, O-glycans, and GSL-glycan
417 solutions were mixed with 2,5-dihydrobenzoic acid and subjected to Matrix-assisted laser
418 desorption/ionization-time of flight mass spectrometry (MALDI-TOF MS). 2AB-labeled
419 GAG disaccharides were analyzed by HPLC. The glycan compositions were manually
420 determined by conducting database searches (i.e., a compositional search of the UniCarbKB

421 database (http://www.unicarbkb.org/query) for fOSs and N- and O-glycans and of the
422 SphinGOMAP database (http://www.sphingomap.org/) for GSL-glycans). All previously
423 deposited GSL-glycans in the SphinGOMAP database were extracted and compiled as an in-
424 house database to allow searching by the m/z value and/or composition. The absolute
425 quantification was obtained by comparative analyses between the MS signal areas derived
426 from each glycan and the internal standard.
427
428 **Statistics**
429 All data in this study are presented as the mean ± standard deviation and were repeated at
430 least three times unless otherwise indicated. Data analysis was performed using GraphPad
431 Prism 9 software version 9.4.1 (GraphPad Software, Inc., San Diego, CA, USA), and the
432 Welch *t*-test/Welch analysis of variance with subsequent use of the Tukey–Kramer multiple
433 comparison tests were used to determine significant differences between the groups. *P*-values
434 <0.05 were considered significant. JMP Pro version 16.2.0 (SAS Institute, Cary, NC, USA)
435 was used to reveal the relationships between each subject of sub glycomes; we performed
436 principal component analysis (PCA) and hierarchical cluster analysis.
437
438 **Study approval**
439 Acquisition and use of patient tissues were approved by the institutional review board (IRB)
440 of Hokkaido University (approval number: 014-0144), and informed consent was obtained in
441 advance. All animal studies were performed according to established ethical guidelines
442 approved by the local animal care committee.
443
444 **Data availability**
445 All data reported in this paper is available from the corresponding author upon request. This

paper does not report original code. Any additional information required to reanalyze the data reported in this paper is available from the lead contact upon request.

ACKNOWLEDGMENTS

We thank the Iwasaki laboratory members for technical support, J. Gu (Tohoku Pharmaceutical University) for the Flox-α1,6 fucosyltransferase (*Fut8*) mouse, Y. Kobayashi (J-OIL MILLS, Inc.) for PhoSL-lectin. This work was funded by the Japan Society for the Promotion of Science KAKENHI (Grant-in-Aid for Challenging Exploratory Research: funding numbers: 16K15650, 19K22672 [to NI]; Grant-in-Aid for Research (B): funding numbers: 22H03917 [to TO]; and Grant-in-Aid for Early-Career Scientists: funding number: 19K18516 [to KH]) and AMED (Grant Number JP22zf01270004h0002 [to NI, TO, KH]).

AUTHOR CONTRIBUTIONS

Conceptualization: NI

Methodology: KH, TO

Investigation: KH, TO, HH, JF, DM, MM, NI

Visualization: KH, HH

Funding acquisition: KH, NI, TO

Project administration: KH, TO, NI

Supervision: TO, NI

Writing – original draft: KH, TO

Writing – review & editing: KH, TO, HH, JF, DM, MM, NI

CONFLICT-OF-INTEREST STATEMENT: The authors have declared that no conflict of interest exists.

471

472

473 **References**

474 1. Grillet B, et al. Matrix metalloproteinases in arthritis: towards precision medicine. *Nat.*
475 *Rev. Rheumatol.* [published online ahead of print: May 2023]; doi:10.1038/s41584-023-
476 00966-w

477 2. Safiri S, et al. Global, regional and national burden of osteoarthritis 1990-2017: a
478 systematic analysis of the Global Burden of Disease Study 2017. *Ann. Rheum. Dis.*
479 2020;79(6):819–828.

480 3. Thorstensson CA, et al. Natural course of knee osteoarthritis in middle-aged subjects with
481 knee pain: 12-year follow-up using clinical and radiographic criteria. *Ann. Rheum. Dis.*
482 2009;68(12):1890–1893.

483 4. Huey DJ, Hu JC, Athanasiou KA. Unlike bone, cartilage regeneration remains elusive.
484 *Science* 2012;338(6109):917–921.

485 5. Glyn-Jones S, et al. Osteoarthritis. *Lancet* [published online ahead of print: March 3,
486 2015]; doi:10.1016/S0140-6736(14)60802-3

487 6. Chu CR. Defining Pre-Osteoarthritis Is Key to Prevention. *Cartilage* 2016;7(2):204.

488 7. Mahmoudian A, et al. Early-stage symptomatic osteoarthritis of the knee - time for
489 action. *Nat. Rev. Rheumatol.* 2021;17(10):621–632.

490 8. Henrotin Y. Osteoarthritis in year 2021: biochemical markers. *Osteoarthritis Cartilage*
491 2021;S1063-4584(21)00960–2.

492 9. Vignon E, et al. Screening of degradative enzymes from articular cartilage in
493 experimental osteoarthritis. *Clin. Rheumatol.* 1987;6(2):208–214.

494 10. Brew CJ, et al. Gene expression in human chondrocytes in late osteoarthritis is changed

495 in both fibrillated and intact cartilage without evidence of generalised chondrocyte
496 hypertrophy. *Ann. Rheum. Dis.* 2010;69(1):234–240.

497 11. Otero M, et al. Human chondrocyte cultures as models of cartilage-specific gene
498 regulation. *Methods Mol. Biol. Clifton NJ* 2012;806:301–336.

499 12. Goldring MB. Chondrogenesis, chondrocyte differentiation, and articular cartilage
500 metabolism in health and osteoarthritis. *Ther. Adv. Musculoskelet. Dis.* 2012;4(4):269–
501 285.

502 13. van Meurs JB, et al. Kinetics of aggrecanase- and metalloproteinase-induced
503 neoepitopes in various stages of cartilage destruction in murine arthritis. *Arthritis*
504 *Rheum.* 1999;42(6):1128–1139.

505 14. Matsuhashi T, et al. Alteration of N-glycans related to articular cartilage deterioration
506 after anterior cruciate ligament transection in rabbits. *Osteoarthritis Cartilage*
507 2008;16(7):772–778.

508 15. Urita A, et al. Alterations of high-mannose type N-glycosylation in human and mouse
509 osteoarthritis cartilage. *Arthritis Rheum.* 2011;63(11):3428–3438.

510 16. Snelling S, et al. A gene expression study of normal and damaged cartilage in
511 anteromedial gonarthrosis, a phenotype of osteoarthritis. *Osteoarthr. Cartil. OARS*
512 *Osteoarthr. Res. Soc.* 2014;22(2):334–343.

513 17. Kobayashi Y, et al. A novel core fucose-specific lectin from the mushroom Pholiota
514 squarrosa. *J. Biol. Chem.* 2012;287(41):33973–33982.

515 18. Wu W, et al. Sites of collagenase cleavage and denaturation of type II collagen in aging
516 and osteoarthritic articular cartilage and their relationship to the distribution of matrix
517 metalloproteinase 1 and matrix metalloproteinase 13. *Arthritis Rheum.*

518 2002;46(8):2087–2094.

519 19. Song R-H, et al. Aggrecan degradation in human articular cartilage explants is mediated
520 by both ADAMTS-4 and ADAMTS-5. *Arthritis Rheum.* 2007;56(2):575–585.

521 20. Malfait A-M, et al. Inhibition of ADAM-TS4 and ADAM-TS5 prevents aggrecan
522 degradation in osteoarthritic cartilage. *J. Biol. Chem.* 2002;277(25):22201–22208.

523 21. Aigner T, et al. Anabolic and catabolic gene expression pattern analysis in normal versus
524 osteoarthritic cartilage using complementary DNA-array technology. *Arthritis Rheum.*
525 2001;44(12):2777–2789.

526 22. Karsdal MA, et al. Cartilage degradation is fully reversible in the presence of
527 aggrecanase but not matrix metalloproteinase activity. *Arthritis Res. Ther.*
528 2008;10(3):R63.

529 23. Reimann I, Christensen SB, Diemer NH. Observations of reversibility of
530 glycosaminoglycan depletion in articular cartilage. *Clin. Orthop.* 1982;(168):258–264.

531 24. Yang Q, Wang L-X. Mammalian α-1,6-Fucosyltransferase (FUT8) Is the Sole Enzyme
532 Responsible for the N-Acetylglucosaminyltransferase I-independent Core Fucosylation
533 of High-mannose N-Glycans. *J. Biol. Chem.* 2016;291(21):11064–11071.

534 25. Toegel S, et al. Glycophenotyping of osteoarthritic cartilage and chondrocytes by RT-
535 qPCR, mass spectrometry, histochemistry with plant/human lectins and lectin
536 localization with a glycoprotein. *Arthritis Res. Ther.* 2013;15(5):R147.

537 26. Yu H, et al. Characterization of aberrant glycosylation associated with osteoarthritis
538 based on integrated glycomics methods. *Arthritis Res. Ther.* 2023;25(1):102.

539 27. Homan K, et al. Alteration of the Total Cellular Glycome during Late Differentiation of
540 Chondrocytes. *Int. J. Mol. Sci.* 2019;20(14):E3546.

541 28. Fujitani N, et al. Total cellular glycomics allows characterizing cells and streamlining
542 the discovery process for cellular biomarkers. *Proc. Natl. Acad. Sci. U. S. A.*
543 2013;110(6):2105−2110.

544 29. Yoshida Y, et al. Quantitative analysis of total serum glycome in human and mouse.
545 *Proteomics* 2016;16(21):2747−2758.

546 30. Furukawa J-I, et al. Impact of the Niemann-Pick c1 Gene Mutation on the Total Cellular
547 Glycomics of CHO Cells. *J. Proteome Res.* 2017;16(8):2802−2810.

548 31. Gao C, et al. Sensitivity of heterozygous α1,6-fucosyltransferase knock-out mice to
549 cigarette smoke-induced emphysema: implication of aberrant transforming growth
550 factor-β signaling and matrix metalloproteinase gene expression. *J. Biol. Chem.*
551 2012;287(20):16699−16708.

552 32. Wang X, et al. Dysregulation of TGF-beta1 receptor activation leads to abnormal lung
553 development and emphysema-like phenotype in core fucose-deficient mice. *Proc. Natl.*
554 *Acad. Sci. U. S. A.* 2005;102(44):15791−15796.

555 33. Gonzalez DS, Jordan IK. The alpha-mannosidases: phylogeny and adaptive
556 diversification. *Mol. Biol. Evol.* 2000;17(2):292−300.

557 34. Ross KA, et al. Comparison of Three Methods to Quantify Repair Cartilage Collagen
558 Orientation. *Cartilage* 2013;4(2):111−120.

559 35. Glasson SS, et al. Deletion of active ADAMTS5 prevents cartilage degradation in a
560 murine model of osteoarthritis. *Nature* 2005;434(7033):644−648.

561 36. Stanton H, et al. Investigating ADAMTS-mediated aggrecanolysis in mouse cartilage.
562 *Nat. Protoc.* 2011;6(3):388−404.

563 37. Estes BT, et al. Isolation of adipose-derived stem cells and their induction to a
564 chondrogenic phenotype. *Nat. Protoc.* 2010;5(7):1294–1311.

565 38. Patwari P, et al. Ultrastructural quantification of cell death after injurious compression
566 of bovine calf articular cartilage. *Osteoarthr. Cartil. OARS Osteoarthr. Res. Soc.*
567 2004;12(3):245–252.

568 39. Rao X, et al. An improvement of the 2ˆ(-delta delta CT) method for quantitative real-
569 time polymerase chain reaction data analysis. *Biostat. Bioinforma. Biomath.*
570 2013;3(3):71–85.

571 40. Ovchinnikov DA, et al. Col2a1-directed expression of Cre recombinase in
572 differentiating chondrocytes in transgenic mice. *Genes. N. Y. N 2000* 2000;26(2):145–
573 146.

574 41. Yamada T, et al. Carminerin contributes to chondrocyte calcification during
575 endochondral ossification. *Nat. Med.* 2006;12(6):665–670.

576 42. Nakamichi Y, et al. Chondromodulin I is a bone remodeling factor. *Mol. Cell. Biol.*
577 2003;23(2):636–644.

578 43. Lufkin T, et al. Homeotic transformation of the occipital bones of the skull by ectopic
579 expression of a homeobox gene. *Nature* 1992;359(6398):835–841.

580 44. Matsui Y, et al. Accelerated development of aging-associated and instability-induced
581 osteoarthritis in osteopontin-deficient mice. *Arthritis Rheum.* 2009;60(8):2362–2371.

582 45. Stoop R, et al. Type II collagen degradation in spontaneous osteoarthritis in C57Bl/6 and
583 BALB/c mice. *Arthritis Rheum.* 1999;42(11):2381–2389.

584 46. Fujitani N, et al. Qualitative and quantitative cellular glycomics of glycosphingolipids
585 based on rhodococcal endoglycosylceramidase-assisted glycan cleavage, glycoblotting-

586 assisted sample preparation, and matrix-assisted laser desorption ionization tandem
587 time-of-flight mass spectrometry analysis. *J. Biol. Chem.* 2011;286(48):41669–41679.

588 47. Takegawa Y, et al. Simultaneous analysis of heparan sulfate, chondroitin/dermatan
589 sulfates, and hyaluronan disaccharides by glycoblotting-assisted sample preparation
590 followed by single-step zwitter-ionic-hydrophilic interaction chromatography. *Anal.*
591 *Chem.* 2011;83(24):9443–9449.

592 48. Furukawa J, et al. Quantitative O-Glycomics by Microwave-Assisted β-Elimination in
593 the Presence of Pyrazolone Analogues. *Anal. Chem.* 2015;87(15):7524–7528.

594 49. Furukawa J, et al. Comprehensive approach to structural and functional glycomics based
595 on chemoselective glycoblotting and sequential tag conversion. *Anal. Chem.*
596 2008;80(4):1094–1101.

597

598 **FIGURES**

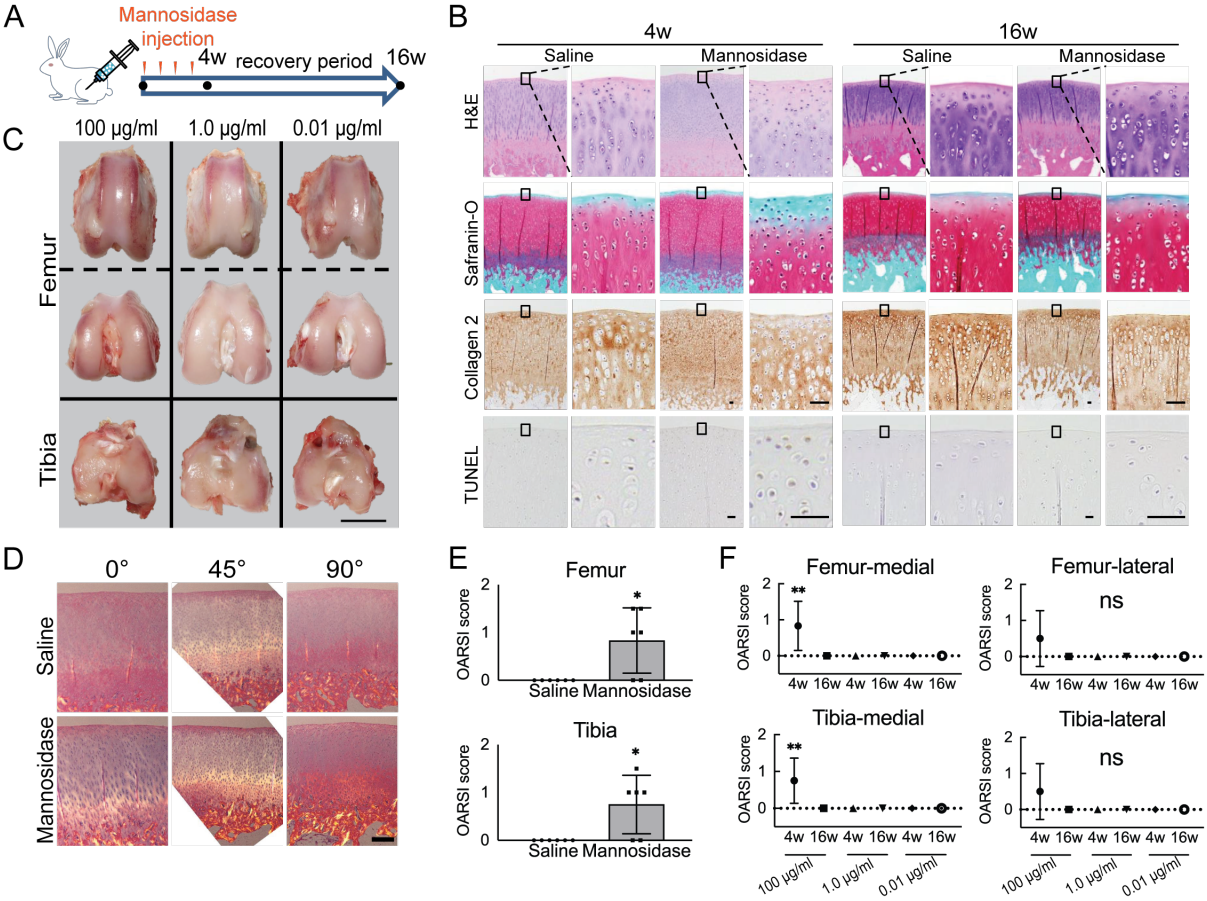

599

600 **Fig. 1. Effects of α-mannosidase injection in the knee joint in vivo.**

601 **(A)** Time course of intra-articular α-mannosidase injection and unloading. Red arrows
602 indicate the one-shot, intra-articular injection that was performed once a week. **(B)**
603 Histological evaluation of knee articular cartilage 4 weeks after intermittent α-mannosidase
604 infusion and 16 weeks after load removal. Scale bars, 50 μm. **(C)** Representative macroscopic
605 assessment of the articular cartilage using mannosidase concentration. Scale bar, 1 cm. **(D)**
606 Evaluation of the collagen orientation of reparative tissues at 4 weeks postoperatively.
607 Sections stained with HE was viewed under a polarized light microscope at multiple angles
608 (0°, 45°, and 90°). Scale bar, 200 μm. **(E)** OARSI scores at 4 weeks postoperatively on
609 sections from the knee joint (n = 6). **(F)** Tissue degeneration scores at each time point are
610 based on mannosidase concentration. Data are shown as mean ± standard deviation. *P <

611 0.05, **$P < 0.01$ versus the saline group in (E), and versus 4 weeks in (F). In (E), the Welch
612 t-test was used for statistical analysis. In (F), n = 6 rabbits per group. One-way analysis of
613 variance with Tukey's multiple comparison test was used to perform statistical analysis. HE,
614 hematoxylin and eosin; OARSI, Osteoarthritis Research Society International; TUNEL,
615 terminal deoxynucleotidyl transferase dUTP nick end labeling.

616

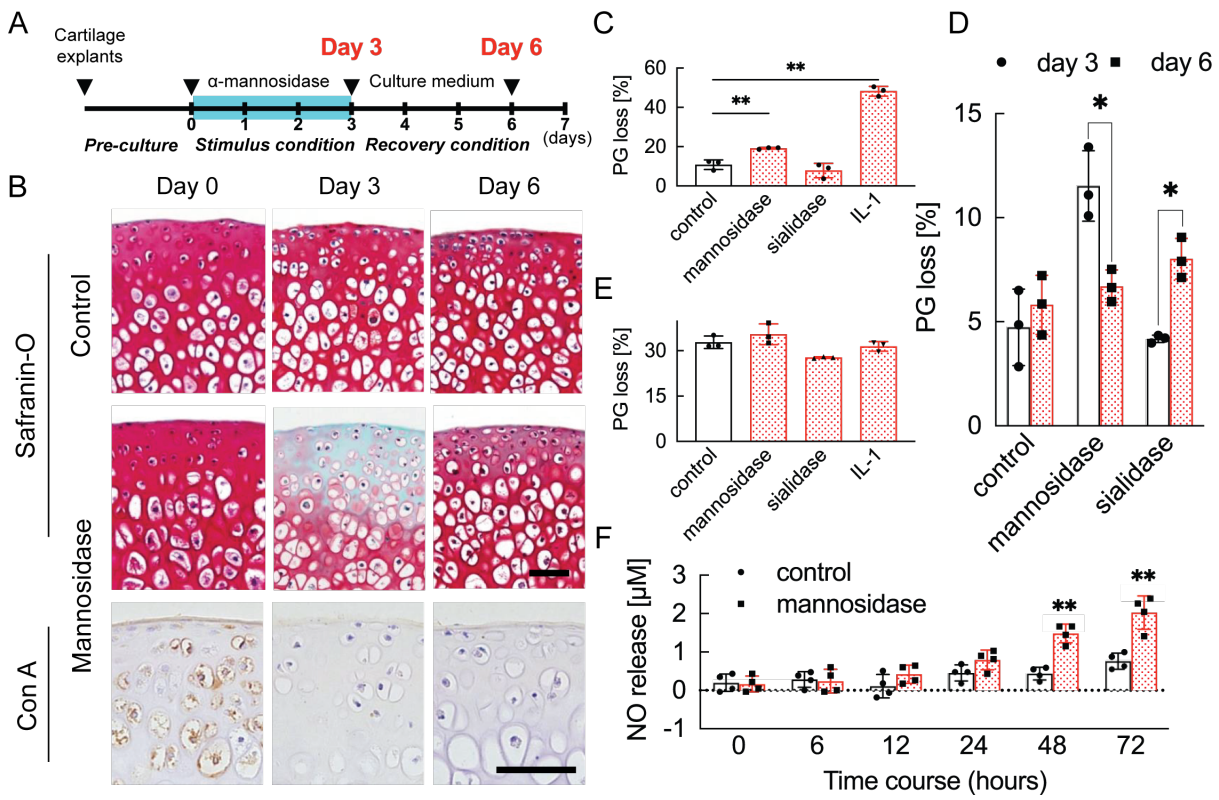

Fig. 2. Cartilage degradation induced by mannosidase stimulation.

(A) Schematic diagram of the procedures used to establish the early OA model before irreversible and progressive destruction of articular cartilage. **(B)** Mannosidase-treated cartilage stained with Safranin O and Con A. The distribution of high-mannose type N-glycans is decreased in mannosidase-induced degraded mouse cartilage. Scale bars, 50 μm. **(C), (D)** PG release after exposure to mannosidase (C) and recovery after its removal from cultured cartilage grafts (D). **(E)** To investigate the non-chondrocyte-mediated release of fragments, PG loss was measured in cartilage explants that had undergone freeze-thaw cycles. **(F)** Sequential NO released into media measured as concentrations of nitrite for cartilage explants stimulated with mannosidase. Data are shown as mean ± standard deviation (s.d.). $*P < 0.05$, $**P < 0.01$ versus the control group in (C), (E), and (F), and versus day 3 in (D). In (C) and (E), n = 3 samples (six mice) per group. One-way ANOVA with the Tukey multiple comparison test was used to perform statistical analysis. In (D), n = 12 mice in each group and n = 3 samples (six mice) at each time point. In (F), n = 16 mice at each time point

632 and n = 4 samples (eight mice) per group. In (D) and (F), two-way ANOVA with the Sidak

633 multiple-comparisons test was used to perform statistical analysis. Con A, concanavalin A;

634 NO, nitric oxide; ANOVA, analysis of variance; PG, proteoglycan.

635

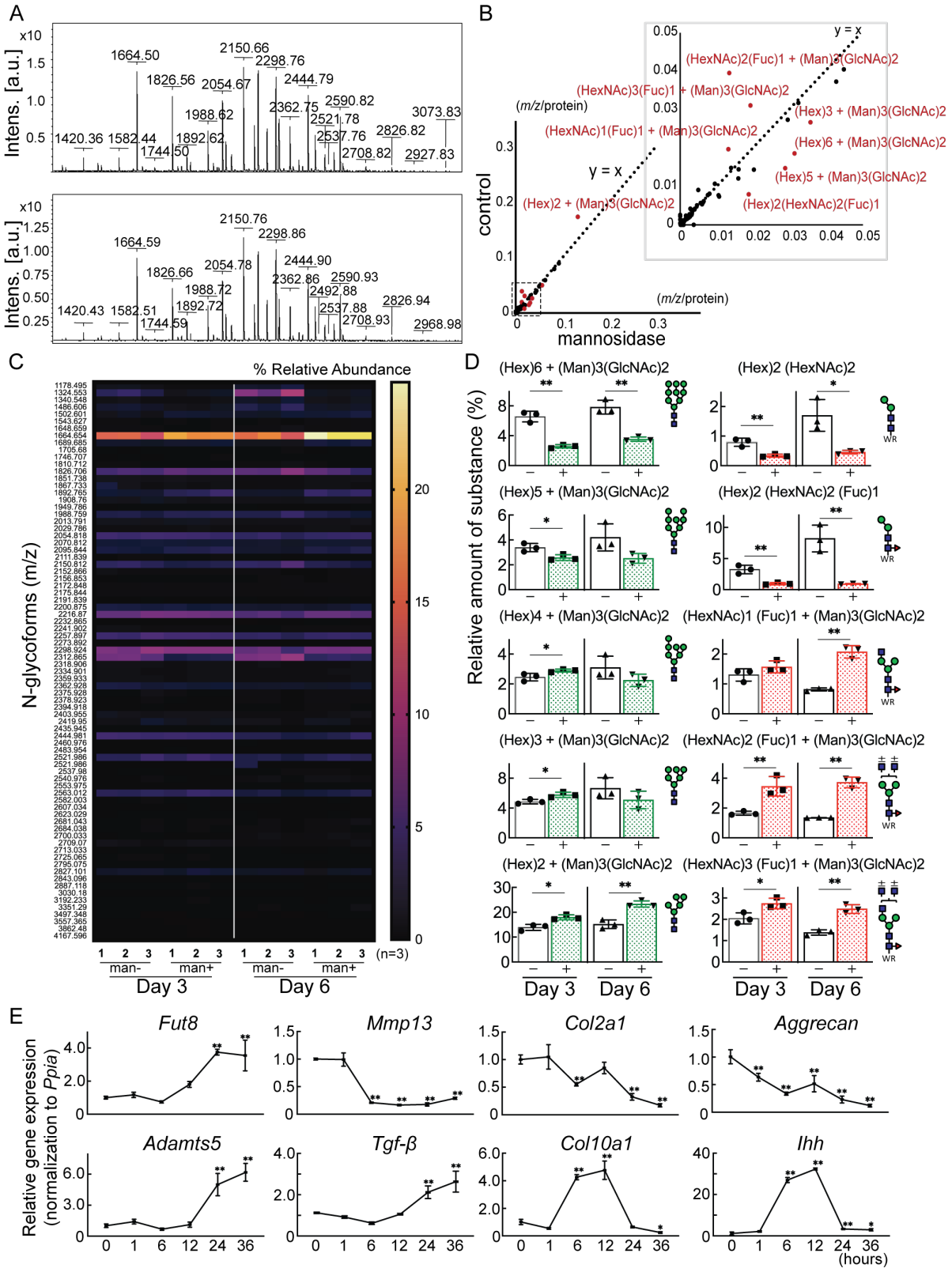

Fig. 3. Cartilage N-glycomes.

(A) MALDI-TOF MS spectra showing the quantitative N-glycan profiles of cartilage before (upper) and after (lower) mannosidase treatment. **(B)** Scatter plot of the changes in *m/z* per

640 protein abundance in the mannosidase (x-axis) and control (y-axis) N-glycan structures. The
641 red dots indicate the top 10 N-glycan structures based on the deviation from the y = x line.
642 **(C)** Heatmap of N-glycome showing differential N-glycan expression in the mannosidase
643 (man+) group versus the control (man-) group. **(D)** N-glycans altered by mannosidase were
644 corefucosylated glycans and high-mannose type N-glycans. **(E)** RT-PCR expression analysis
645 of marker genes in organ culture of cartilage with mannosidase. Data are shown as mean ±
646 standard deviation. *$P < 0.05$, **$P < 0.01$ versus the control group in (D), and versus 0 hours
647 in (E). In (D) and (E), n = 3 samples (six mice) per group. In (D), unpaired t-tests were used
648 to perform statistical analyses. In (E), one-way ANOVA with the Dunnett multiple
649 comparison test was used to perform statistical analysis. MALDI-TOF MS, matrix-assisted
650 laser desorption/ionization-time of flight mass spectrometry; ANOVA, analysis of variance;
651 RT-PCR, real-time polymerase chain reaction.

652

653

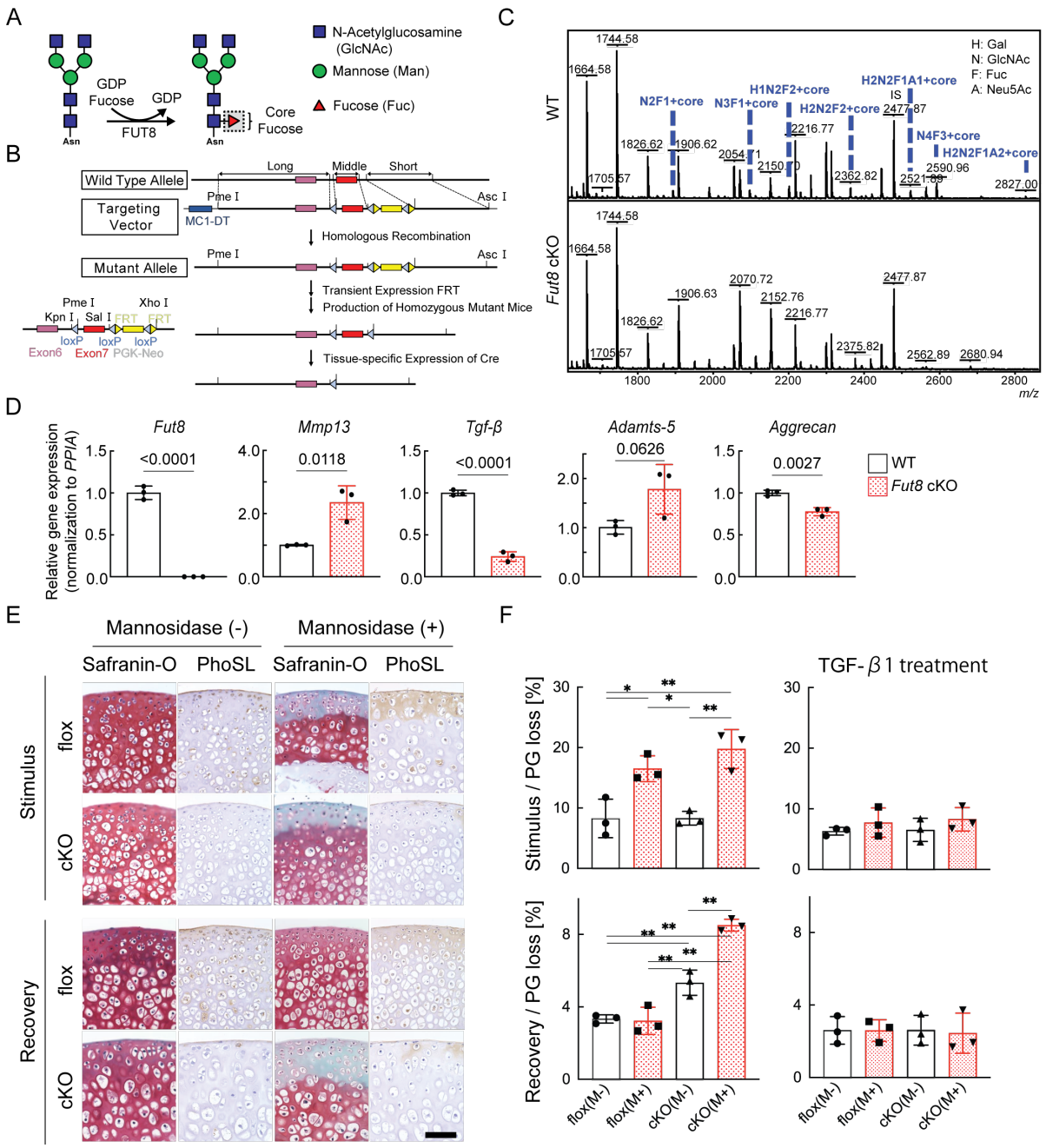

654

655 **Fig. 4. Loss of resilience due to FUT8 deficiency in cartilage.**

656 **(A)** Biological reaction of FUT8. FUT8 transfers fucose to the innermost GlcNAc residue of

657 complex N-glycans via α1,6-linkage (corefucosylation). **(B)** Targeted disruption of *Fut8*

658 locus. The *Fut8* gene (WT allele; top), targeting vector (middle), and disrupted *Fut8* locus

659 (mutant allele; bottom). Schematic representation of the *Fut8*-targeting strategy and Cre-
660 mediated recombination of the *Fut8*^{loxP} allele. (**C**) MALDI-TOF MS mass spectra of N-
661 glycans from WT and *Fut8* cKO mice. The corefucosylation levels in cartilage were
662 decreased and undetectable in *Fut8* cKO mice. (**D**) Gene profile in chondrocytes isolated
663 from *Fut8* cKO mice. The expression levels of these genes in WT cells were set to 1. PPIA,
664 peptidylprolyl isomerase A. (**E**) Histological findings in cartilage explants from *Fut8* cKO
665 mice and their floxed littermates cultured with mannosidase and subjected to Safranin O
666 staining and PhoSL lectin staining. Scale bar, 50 μm. (**F**) PG release in cultured cartilage
667 explants from *Fut8* cKO mice and their floxed littermates. M-, Mannosidase (-); M+,
668 Mannosidase (+). Data are shown as mean ± standard deviation. In (F), n = 3 samples (six
669 mice) per group. *$P < 0.05$, **$P < 0.01$. One-way ANOVA, with the Tukey multiple
670 comparison test, was used to perform statistical analysis. MALDI-TOF MS, matrix-assisted
671 laser desorption/ionization-time of flight mass spectrometry; WT, wild-type; cKO,
672 conditional knockout; PG, proteoglycan; ANOVA, analysis of variance.

673

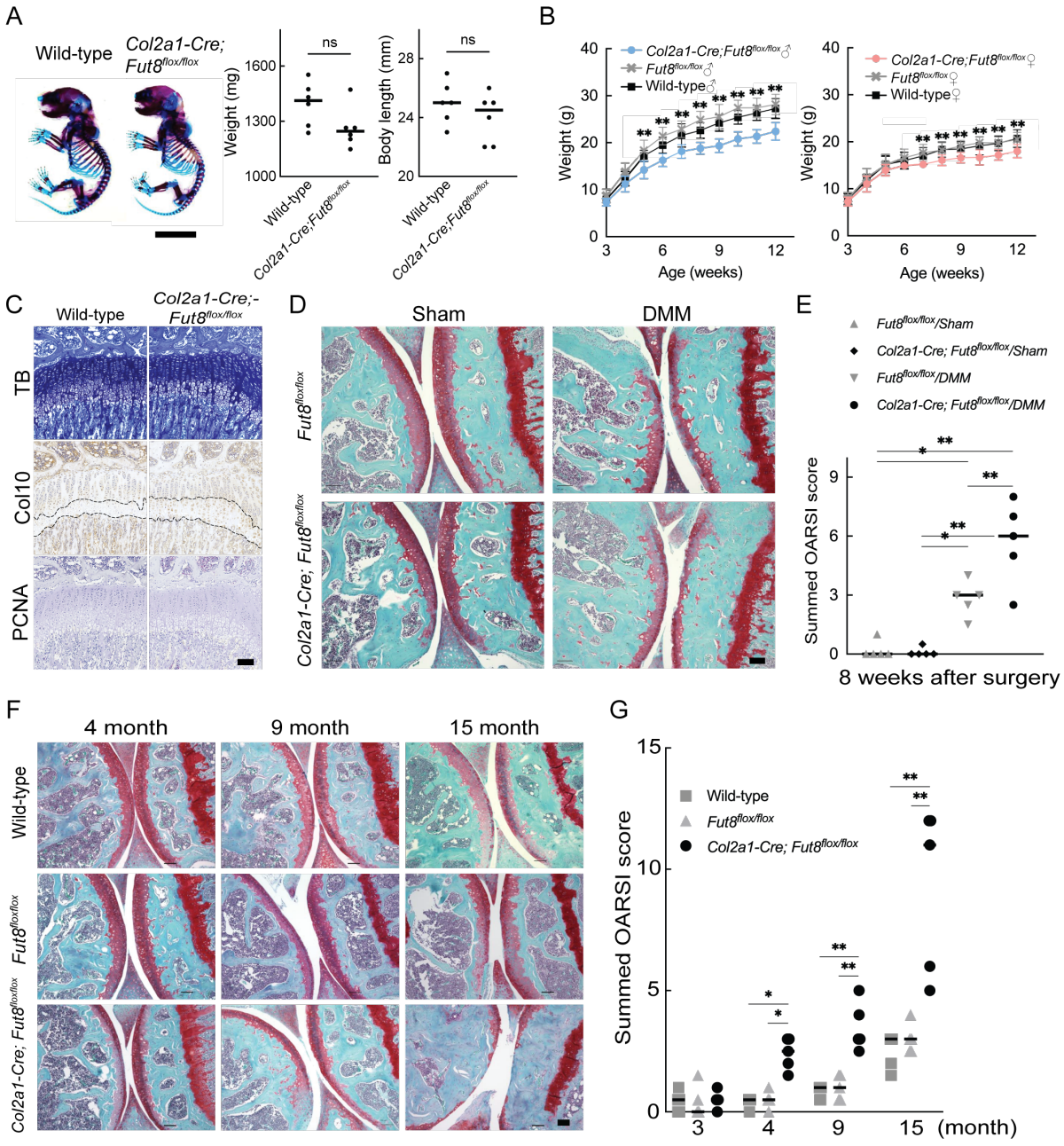

Fig. 5. OA acceleration in *Fut8* cKO mice.

(A) Double staining with alizarin red and alcian blue of the whole skeleton of wild-type and *Col2a1-Cre;Fut8*$^{flox/flox}$ cKO littermate embryos (newborn). Scale bars, 1 cm (left). Weight and body length of wild-type and cKO littermate embryos (right). **(B)** Growth curves were determined by body weight in male (left) and female (right) wild-type mice and their cKO littermates. **(C)** Histologic findings in knee joints from 4-week-old mice. Toluidine blue (TB) staining and immunostaining for type X collagen (Col10) and proliferating cell nuclear

682 antigen (PCNA) in growth plates of the tibia were performed in each mouse genotype. The
683 dashed line indicates the hypertrophic zone. Scale bar, 100 μm. **(D)**, **(E)** Features of
684 instability-induced OA in *Fut8*$^{flox/flox}$ (flox) mice and their cKO littermates 8 weeks after
685 surgery. Safranin O staining is shown for each mouse genotype. Scale bar, 100 μm (D).
686 Summed histological scores for OA severity in the knee cartilage from flox and cKO mice, as
687 determined using the OARSI scoring system, are shown (E). **(F)**, **(G)** Features of age-
688 associated osteoarthritis in wild-type mice and their flox and cKO littermates. Safranin O
689 staining of the knee joint is shown for each mouse genotype at 3, 4, 9, and 15 months of age.
690 Scale bar, 100 μm (F). The summed OARSI scores are shown (G). Data are shown as mean ±
691 standard deviation. In (A), the Welch t-test was used to perform statistical analyses (n = 6
692 mice per group). In (B), n = 15 mice per group at each time point. In (E) and (G), n = 5 mice
693 per group at each time point. *$P < 0.05$, **$P < 0.01$ versus the wild-type group in (B) and
694 (G), and versus flox mice in (E). One-way ANOVA with the Tukey multiple comparisons test
695 (B), and two-way ANOVA with the Tukey multiple comparisons test (E and G) were used to
696 perform statistical analysis. OA, osteoarthritis; cKO, conditional knockout; OARSI,
697 Osteoarthritis Research Society International. ANOVA, analysis of variance; ns, not
698 significant.

699

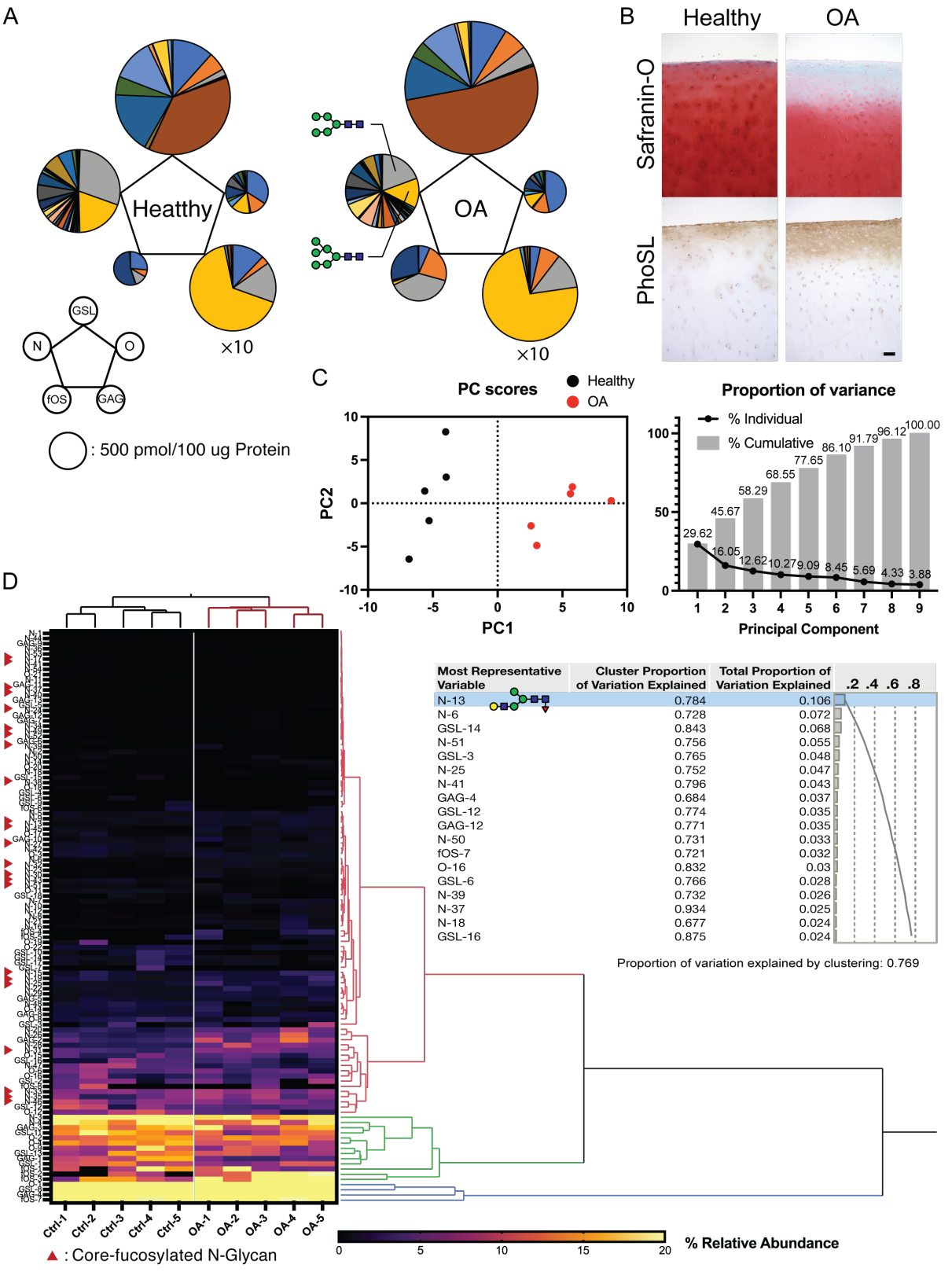
A
Heatthy
OA
×10
×10
GSL
N
O
fOS
GAG
: 500 pmol/100 ug Protein
B
Healthy
OA
Safranin-O
PhoSL
C
PC scores
Healthy
OA
PC2
PC1
Proportion of variance
% Individual
% Cumulative
29.62
45.67
58.29
68.55
77.65
86.10
91.79
96.12
100.00
16.05
12.62
10.27
9.09
8.45
5.69
4.33
3.88
Principal Component
D
Most Representative Variable
Cluster Proportion of Variation Explained
Total Proportion of Variation Explained
N-13 0.784 0.106
N-6 0.728 0.072
GSL-14 0.843 0.068
N-51 0.756 0.055
GSL-3 0.765 0.048
N-25 0.752 0.047
N-41 0.796 0.043
GAG-4 0.684 0.037
GSL-12 0.774 0.035
GAG-12 0.771 0.035
N-50 0.731 0.033
fOS-7 0.721 0.032
O-16 0.832 0.03
GSL-6 0.766 0.028
N-39 0.732 0.026
N-37 0.934 0.025
N-18 0.677 0.024
GSL-16 0.875 0.024
Proportion of variation explained by clustering: 0.769
Ctrl-1
Ctrl-2
Ctrl-3
Ctrl-4
Ctrl-5
OA-1
OA-2
OA-3
OA-4
OA-5
▲ : Core-fucosylated N-Glycan
% Relative Abundance

700

Fig. 6. Altered glycosylation of human Osteoarthritis (OA) cartilage based on comprehensive glycan analysis.

(A) Total glycome profiling of human OA cartilage. Pie charts at the vertices of the pentagon correspond to the glycan expression profiles of N-glycans, O-glycans, GSL-glycans, free oligosaccharides (fOS), and glycosaminoglycan (GAG). The size of each circle and its constituent colors reflect the absolute quantity of glycans (pmol/100 μg protein) and the glycan substructures, respectively. The sizes of the circles representing the GAG contents are decreased by 1/10-fold. Each color indicates the estimated glycan structure and corresponds to the respective glycan number in the S3 Table. **(B)** Expression of core fucose in healthy and OA cartilage. Scale bar, 100 μm. **(C)** Principal component analysis (PCA) of a glycan expression data set. Data points represent individual samples. The first principal component (PC1) distinguishes healthy and OA samples. **(D)** Hierarchical cluster analysis results showing cluster image display for total glycans with color gradient for relative glycan expression and dendrogram for each glycan structure. Cluster summary of PCA on the glycome are shown on the right. The most representative variable is (Hex)1 (HexNAc)1 (Fuc)1 + (Man)3(GlcNAc)2 which means the largest squared correlation with its cluster component.

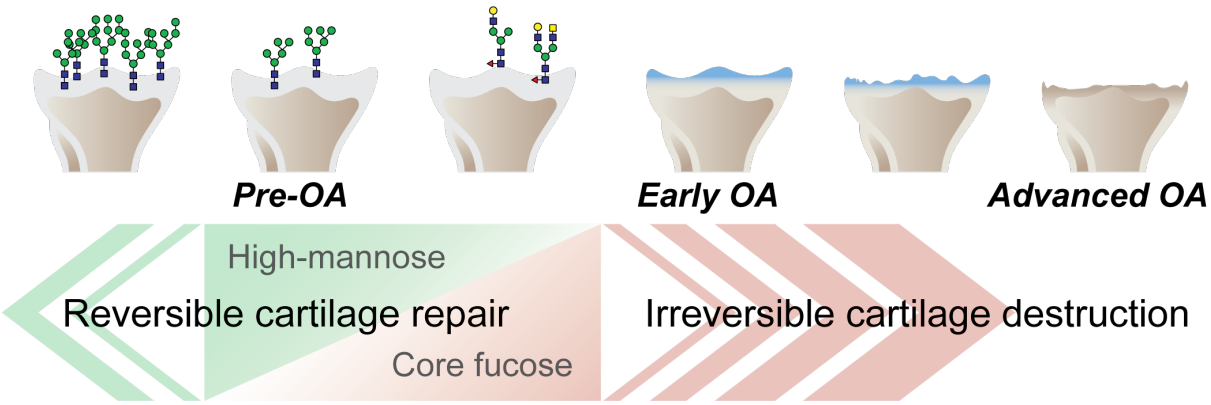

720 **Fig. 7. Graphical abstract.**

721 The corefucosylation of N-glycans is associated with the reduction of high-mannose type N-
722 glycans in articular cartilage functions to maintain the formed vitreous cartilage as cartilage.
723 Failure of the complementary relationship leads to irreversible cartilage degeneration and
724 destruction of cartilage integrity.

725